

## Article

# A V2G Enabled Bidirectional Single/Three-Phase EV Charging Interface Using Modular Multilevel Buck PFC Rectifier

Anekant Jain <sup>1,\*</sup>, Krishna Kumar Gupta <sup>1</sup>, Sanjay K. Jain <sup>1</sup>, Pallavee Bhatnagar <sup>2</sup> and Hani Vahedi <sup>3</sup>

<sup>1</sup> Thapar Institute of Engineering and Technology, Patiala 147004, India; krishna.gupta@thapar.edu (K.K.G.); skjain@thapar.edu (S.K.J.)

<sup>2</sup> IES College of Technology, Bhopal 462044, India; pallaveebhatnagar9@gmail.com

<sup>3</sup> Dcbel Inc., Montreal, QC H3C 2G9, Canada; hani.vahedi@ieee.org

\* Correspondence: ajain\_phd19@thapar.edu

**Abstract:** The battery charging power electronics interface of an electric vehicle (EV) must be capable of bidirectional power flow to enable both grid-to-vehicle (G2V) and vehicle-to-grid (V2G) operations. In the presence of a single/three-phase AC supply, the front-end of the EV charger employs a power factor correction (PFC) rectifier, which should have the bidirectional capability to facilitate V2G mode. A conventional active rectifier functions in boost mode while performing PFC and voltage regulation. In most of the currently available EVs, however, the battery nominal voltage is low and, hence, a downstream high step-down DC-DC converter and high voltage DC bus capacitor are required in the charging interface. To overcome these issues, this work proposes a bidirectional AC-to-DC buck rectifier topology that can operate in G2V and V2G modes, both in single- and three-phase versions. The proposed topology utilizes the switched capacitors principle to achieve self-balancing of voltages in the capacitors. In addition, it is highly modular in structure. This paper describes the proposed topology, its working and modulation and its applications. The hardware proto model is used to validate the proposed power converter and the control approach to achieve PFC and voltage regulation. In addition, a comparison with other topologies is presented to demonstrate its competence.

**Keywords:** buck rectifier; electric vehicle charging; modular; multilevel; power factor correction; single-phase; three-phase; vehicle-to-grid



**Citation:** Jain, A.; Gupta, K.K.; Jain, S.K.; Bhatnagar, P.; Vahedi, H. A V2G Enabled Bidirectional Single/Three-Phase EV Charging Interface Using Modular Multilevel Buck PFC Rectifier. *Electronics* **2022**, *11*, 1891. <https://doi.org/10.3390/electronics11121891>

Academic Editor: Domenico Mazzeo

Received: 27 April 2022

Accepted: 14 June 2022

Published: 16 June 2022

**Publisher's Note:** MDPI stays neutral with regard to jurisdictional claims in published maps and institutional affiliations.



**Copyright:** © 2022 by the authors. Licensee MDPI, Basel, Switzerland. This article is an open access article distributed under the terms and conditions of the Creative Commons Attribution (CC BY) license (<https://creativecommons.org/licenses/by/4.0/>).

## 1. Introduction

Electric vehicles (EVs) are now considered to be one of the most important breakthroughs in automobile technology. Propelled by the societal concern for environmental pollution, subsidies offered by various governments and rapidly advancing battery technology, the penetration of EVs is growing at an exponential rate. As a result, a widespread energy-efficient charging infrastructure is required to alleviate the range anxiety [1]. An EV charging system's power electronics interface typically consists of two stages: a power factor correction (PFC) rectifier stage and a DC-to-DC converter [2]. Depending on the power needs, these charging systems are powered by a single-phase or three-phase AC power supply [3]. For example, a single-phase AC supply is used for a charging power ranging from 2 kW to 8 kW (usually rated at 32 A) in level-2 on-board EV battery charging, while a three-phase AC supply is used for a charging power of 19.2 kW (generally rated at 80 A) [3]. A three-phase power supply is also used for the off-board EV charging system, and it is specifically designed for the charging station. Various charging levels and their associated powers are summarized in Table 1.

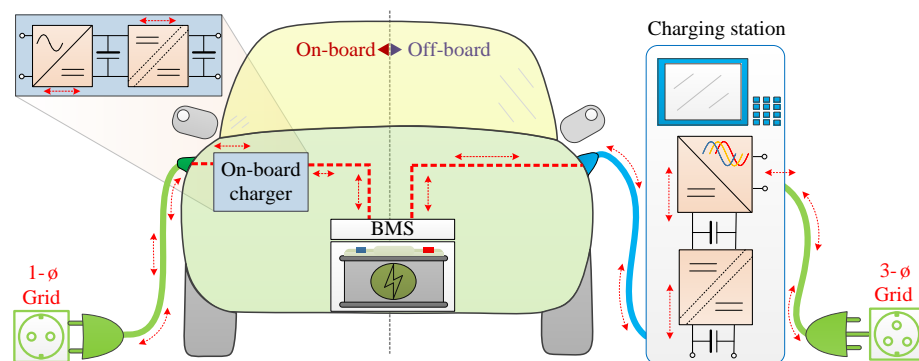
**Table 1.** Charging power levels, type and supply interface for EV charging [3].

Power Level	Charger Type	Input Supply	Supply Interface	Power Level
Level-1	On-board single-phase	120 V RMS	Convenience outlet	1.4 kW (12 A) 2 kW (20 A)
Level-2	On-board Single/three-phase	230 V RMS	Dedicated charging point	8 kW (32 A) 19.2 kW (80 A)
Level-3	Off-board three-phase	415 V RMS	Dedicated charging station	50 kW–200 kW

In modern power systems, EVs offer several advantages, such as peak power regulation, peak load shifting, reduced environmental pollution and so on. EVs can act either as load or as generator, respectively, in grid-to-vehicle (G2V) charging mode and vehicle-to-grid (V2G) discharging mode [4,5]. The power converter employed in “G2V-only” systems is unidirectional in general, which include both normal and fast charging systems. Fast charging puts a strain on the grid network due to the high-power flow [6]. If the G2V charger does not use state-of-the-art conversion, grid disturbances such as unwanted peak loads, harmonics, and low power factor may occur. The V2G system facilitates energy injection back to the grid. An essential constituent of the V2G interface is the grid-connected AC-to-DC converter, which enforces a sinusoidal input current with a high-power factor (close or equal to unity) and enables bidirectional power flow [7].

This work describes the conceptualization, design and validation of a single phase on-board and three-phase off-board bidirectional EV charger that can perform both the functions of charging the vehicle battery and providing active power support to the utility grid [8]. A schematic diagram of the proposed work is shown in Figure 1 and consists of two stages:

1. A switched capacitors (SC) based bidirectional modular AC-to-DC buck PFC active rectifier; and
2. A bidirectional DC-to-DC converter.

**Figure 1.** A simplified structure of single phase (on-board) and three-phase (off-board) bidirectional EV charging.

In two-stage EV charging systems, the input grid power is first converted to a stable DC output voltage using an AC-to-DC converter [9]. In the case of three-phase boost rectifiers (e.g., the conventional active rectifier comprising three legs of complementary power switches) with an input voltage of 415 V RMS, the output voltage ranges from 700 VDC to 800 VDC, which is too high to directly feed the DC-bus of EVs. In the second stage, a DC-to-DC step-down converter is required to reduce this voltage to a nominal voltage suitable for EV battery charging [10]. In this configuration, the total standing voltage (TSV) of the power switches of the rectifier and the DC-DC converter reaches the

same level as the DC-link voltage [11]. Additionally, a high-voltage DC-bus capacitor is used in such a configuration. This work, on the other hand, proposes a buck rectifier at the first stage itself. The schematic of the work, differentiating with the existing topology, is shown in Figure 2. Because the EV battery voltage ranges from 48 V to 400 V, such power electronics interfaces can support batteries ranging from 48 V (e-bikes) to 400 V (PHEV) [12], with the ability to charge the battery in both constant current and constant voltage modes, depending on the battery's state-of-charge (SOC). For this reason, the proposed work offers attractive topological characteristics which are suitable for EV charging applications. The "buck" operation at the rectifier stage is achieved by using a novel class of multilevel topologies which utilize switched capacitors (SCs) principle. The basic idea of the presented SCs-based multilevel rectifier (MLR) is derived from an SCs-based multi-level inverter (MLI), which has recently gained huge popularity [13]. As the SCMLI, which operates with a DC source and an AC load, results in a voltage boost, the SCMLR (operating with an AC source and DC load) is expected to perform buck operation while providing a wide output range. The proposed SCs-based MLR topology has been implemented as a seven-level converter, though it is highly modular and can be easily scaled up. The typical voltage ranges in the conventional and proposed topologies are also indicated in Figure 2, considering an input three-phase AC supply with an RMS value of 415 V. It can be seen that with a step-down factor of 3, the output voltage of the proposed rectifier can be regulated in the range of 195 V to 587 V.

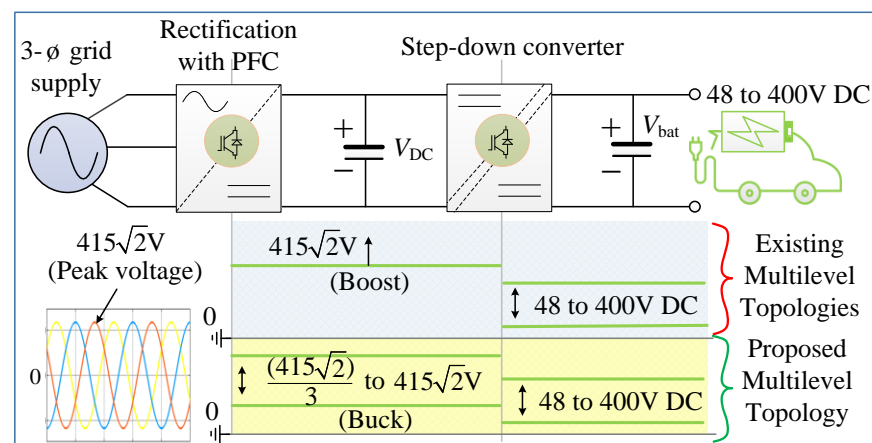


**Figure 2.** A general representation of voltage levels in two-stage EV charging interface with the conventional and proposed rectifier topologies.

In view of the factors related to nominal voltage of EV batteries, advantages of V2G operation and number of phases in the AC supply system, the most desirable criteria for a PFC rectifier topology are: (1) it should accomplish buck operation with a wide output range; (2) it should allow a bidirectional flow of power; and (3) its structure should be straightforward to extend for a three-phase AC input.

Now, as far as multilevel rectifiers (MLRs) are concerned, their classification is shown in Figure 3. The PFC MLRs are broadly classified as single and three-phase topologies. These rectifiers are further classified as buck and boost rectifiers. Non-multilevel topologies with buck or boost modes of operation are characterized by discontinuous conduction mode (DCM) [14], thereby requiring bigger inductive and capacitive filters on the DC and AC sides, respectively [15]. Furthermore, the high-frequency operation of DCM topologies significantly increases the switching losses [16]. Another technique to produce a buck DC voltage is to use a diode bridge and a DC-to-DC buck converter, but such systems show disadvantages in terms of lower efficiency, larger power losses, and higher production costs for medium and high-power applications [17]. In another category of single/three-phase PFC converters, multilevel rectifiers (MLRs) are an emerging class. MLRs allow a bidirectional power flow and minimize the harmonics of the input voltage. These types

of converters are advantageous over the two-level converters because they use lower-voltage-rated power switches, they synthesize higher-quality voltage waveform, they cause reduced  $dv/dt$  stress across the switches and cause much lower THD in the line current [18]. As a result, with the increase in the number of voltage levels, the distortion in input voltage decreases and a filter of the lower size is required.

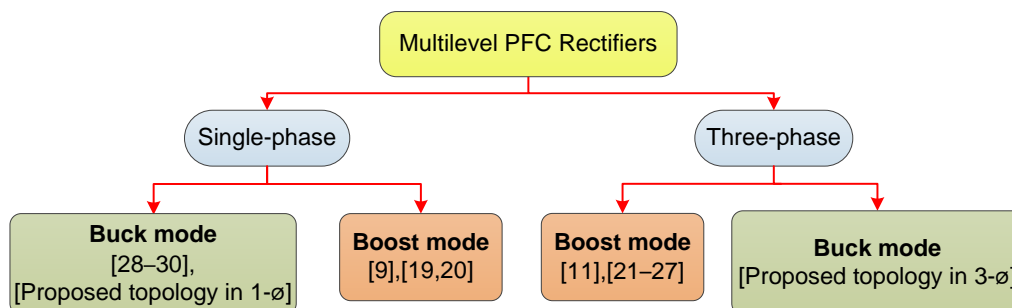


**Figure 3.** Classification of multilevel PFC rectifiers [9,11,19–30].

A boosted output voltage is obtained by using conventional MLR topologies such as cascaded H-bridge (single-phase), neutral point clamped and flying capacitors (single and three-phase) [9,19,20]. Other emerging topologies of three-phase multilevel PFC rectifiers [11,21–27] also operate in boost mode. When applied to the EV charging interface, the main challenges posed by MLRs are: (i) conventional MLRs operate as boost rectifiers; (ii) a high voltage DC-link capacitor is required in-between; and (iii) the capacitors in the MLR topologies require complex methodologies for voltage balancing.

There is limited literature available for the multilevel buck rectifier category, and all can operate in single-phase mode [28–30]. These rectifiers' continuous-conduction mode (CCM) generate a multilevel voltage waveform at the input. Commonly utilized AC-side capacitive and DC-side inductive filters are eliminated due to CCM functioning. The buck rectifier proposed in [28] is based on the cascaded H-bridge (CHB) architecture and has several DC outputs. On the AC side, each module in the CHB structure must interact with the others to produce an almost sinusoidal current in phase with the grid voltage. Each capacitor's voltage must be controlled and regulated on the DC side. Multiple sensors and a complicated control method are required to balance the capacitor output voltage. Topologies [29,30] have been implemented as multioutput and bidirectional five-level and nine-level buck rectifiers, respectively. The three-phase version of these topologies cannot be directly obtained by extending the basic structure of single-phase versions. Additionally, multiple sensors are required to construct a control mechanism to regulate the DC bus capacitors' output voltage. Additionally, to the best of authors' knowledge, no published literature is available on three-phase multilevel buck rectification.

In this work, a novel switched-capacitors-based MLR topology is presented to alleviate the aforesaid limitations. The proposed topology for PFC rectification offers the following characteristics:

- The proposed topology can be easily structured for both the single-phase version (for on-board EV charging) and the three-phase version (for off-board EV charging);
- It operates in both V2G and G2V modes;
- It synthesizes seven levels at the line voltage, thereby considerably improving the harmonic profile. If needed, the modularity of the proposed structure allows further extension of the number of levels;
- Without using any complex control methods, only the output voltage needs to be balanced, and all other capacitors' voltages are automatically balanced;
- It works in buck mode, with a wide output range; and
- It operates in continuous conduction mode, thereby eliminating the need for large filters.

The operation of the proposed topology, voltage and current controllers and level-shifted pulse-width modulation (LSPWM) technique for generating the gate pulses are

explained in the subsequent sections. Experimental testing is carried out for steady-state and dynamic circumstances to verify the proposed work and the results are presented in this article.

### 2. Circuit Topology

The proposed three-phase switched-capacitor-based buck rectifier (SCMBR) is shown in Figure 4. All three phases have a similar power circuit configuration, and an AC line voltage source powers them. The DC-bus capacitor,  $C_o$  supply to the load where the capacitor voltage is to be balanced at  $V_{DC}$ . Each phase of the proposed rectifier has two SC units inserted. The SC units consist of eight switches and two capacitors.

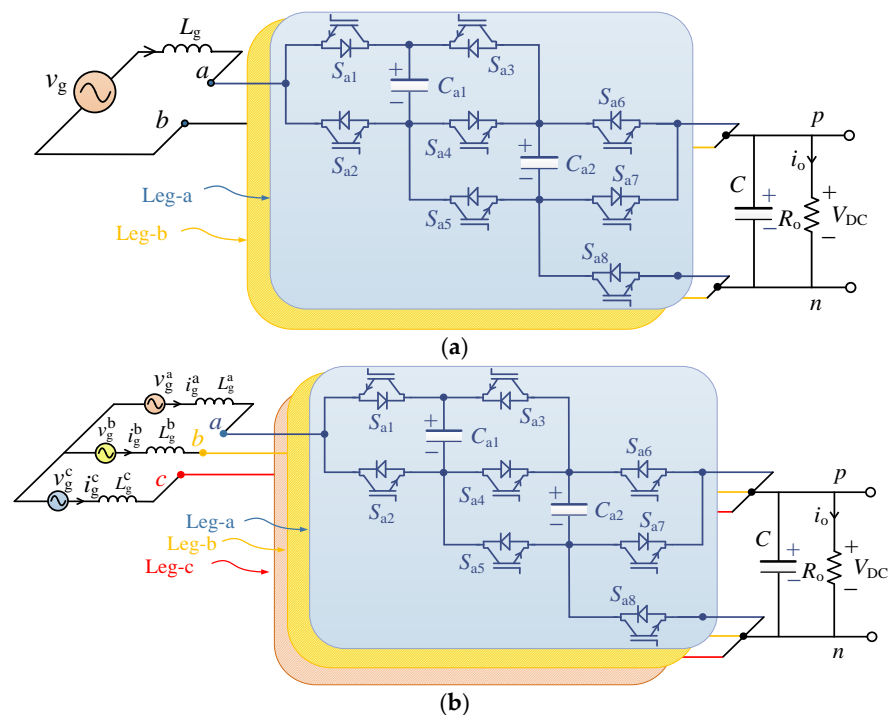


**Figure 4.** Proposed PFC rectifier topology with the capability of bidirectional power flow (a) Single-phase, (b) Three-phase.

At the input terminals of the rectifier, the proposed structure generates four levels as the pole voltage, and it synthesizes seven levels in the line voltages. In each phase, three pairs of complementary power switches and one pair required the same gate pulse, which is to say, if ‘1’ refers to ON state of a switch and ‘0’ refers to the OFF state, the switching functions {where  $x \in a, b, c$ } are:

$$\begin{aligned} \overline{S_{x2}} &= 1 - S_{x1} \\ \overline{S_{x4}} &= 1 - S_{x3} \\ \overline{S_{x7}} &= 1 - S_{x6} \\ S_{x5} &= S_{x8} \end{aligned}$$

Each phase thus generates four levels in the voltage  $V_{xn}$  [ $x \in a, b, c$ ]:  $0, +V_{DC}, +2 V_{DC}$  and  $+3 V_{DC}$ . The switching states of the proposed rectifier are shown in Table 2. Where the switch ON and OFF represents 1 and 0. Capacitors  $C_{x1}, C_{x2}$  and  $C_o$  are to be maintained at a voltage equal to  $V_{DC}$ . At the point of the input terminal, the voltage  $V_{xn}$  can be expressed as:

$$V_{xn} = (S_{x1} + S_{x4} + S_{x7})V_{DC} \tag{1}$$

**Table 2.** Switching states of the proposed three-phase rectifier.

States	Switches				Capacitors			Pole Voltage
	$S_{x1}$	$S_{x3}$	$S_{x5}$	$S_{x6}$	$C_{x1}$	$C_{x2}$	$C_o$	$V_{xn}$
1	0	1	1	1	Charging	Charging	Discharging	0
2	1	1	1	1	Discharging	Discharging	Charging	$+V_{DC}$
3	1	0	0	1	Charging	Neutral	Charging	$+2 V_{DC}$
4	1	0	0	0	Charging	Charging	Charging	$+3 V_{DC}$

Various switching states for the proposed rectifier are described herewith:

1. State 1 ( $V_{xn} = 0$ ): During this state, the switches  $S_{x2}$ ,  $S_{x3}$ ,  $S_{x5}$ ,  $S_{x6}$  and  $S_{x8}$  are turned ON, so as to achieve two simultaneous conduction paths, as shown in Figure 5a. In the path shown with red, it can be seen that all capacitors are bypassed, such that the voltage  $V_{xn} = 0$ . Additionally, for the path shown in green, the capacitors  $C_{x1}$ ,  $C_{x2}$  and  $C_o$  are in parallel and maintain capacitor voltage to  $V_{DC}$ .
2. State 2 ( $V_{xn} = +V_{DC}$ ): During this state, the switches  $S_{x1}$ ,  $S_{x3}$ ,  $S_{x5}$ ,  $S_{x6}$  and  $S_{x8}$  are turned ON, so as to achieve two simultaneous conduction paths, as shown in Figure 5b. In the path shown with red, it can be seen that the capacitor  $C_o$  is in the path with terminal “x” and “n”, such that the voltage  $V_{xn} = +V_{DC}$ . Additionally, for the path shown in green, the capacitors  $C_{x1}$ ,  $C_{x1}$  and  $C_o$  are in parallel and balance the voltage of the capacitor to  $V_{DC}$ .
3. State 3 ( $V_{xn} = +2 V_{DC}$ ): During this state, the switches  $S_{x1}$ ,  $S_{x4}$ , and  $S_{x6}$  are turned ON, so to achieve conduction paths, as shown in Figure 5c. In the path shown with red, it can be seen that the capacitors  $C_{x1}$  and  $C_o$  are in the path with terminal “x” and “n”, such that the voltage  $V_{xn} = +2 V_{DC}$ .
4. State 4 ( $V_{xn} = +3 V_{DC}$ ): During this state, the switches  $S_{x1}$ ,  $S_{x4}$ , and  $S_{x7}$  are turned ON, so as to achieve conduction paths, as shown in Figure 5d. In the path shown with red, it can be seen that the capacitors  $C_{x1}$ ,  $C_{x2}$  and  $C_o$  are series, such that the voltage  $V_{xn} = +3 V_{DC}$ .

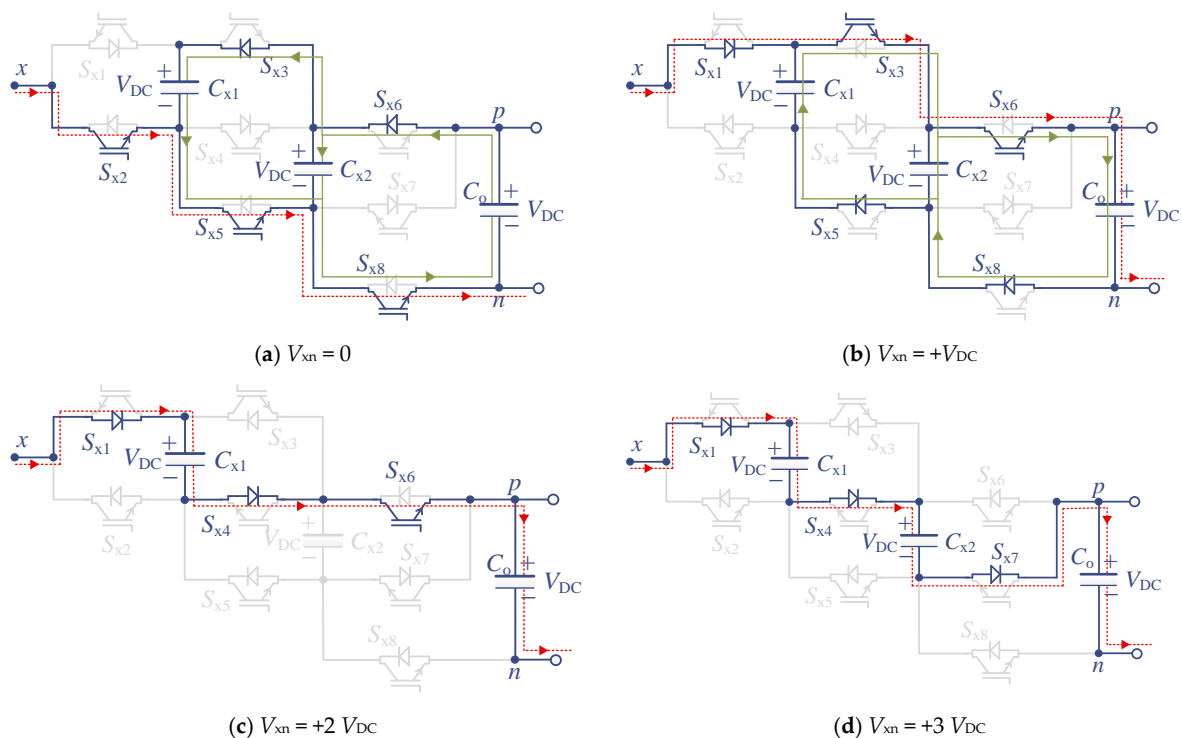


**Figure 5.** Switching states of the proposed topology.

Due to the simple structure, the proposed topology can be presented in a modular approach to increase the number of levels and reduce the gain. Figure 6 shows the n-module where each module consists of 3 switches and one capacitor, and the output voltage gain is  $1/(n + 1)$ .

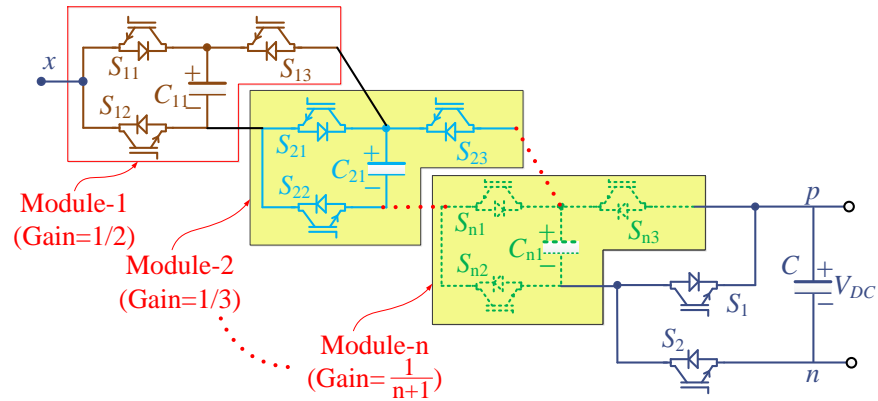


Figure 6. Modular structure of the proposed topology.

The modulation procedure to generate the gate pulses for the switches is discussed in the next section.

### 3. Modulation Scheme and Controller

#### 3.1. Pulse Width Modulation (PWM) Scheme

To regulate the output voltage of the proposed MLR, several modulation schemes such as multicarrier PWM and space vector PWM can be used. The level shifted-PWM (LSPWM) method is used in this work to demonstrate the operation of the proposed MLR and is shown in Figure 7. Each phase uses three high-frequency level-shifted carrier signals and one sinusoidal reference signal [31].

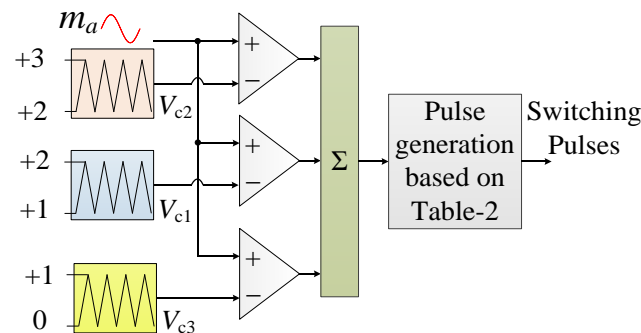
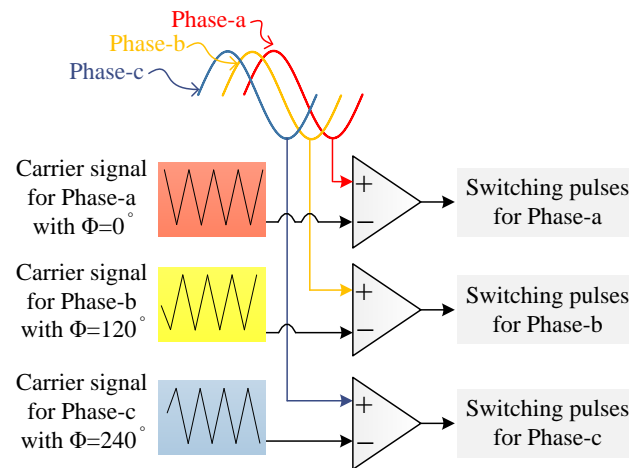


Figure 7. Level shifted PWM signals for phase-a.

For the three-phase operation, there is a need to shift carrier signals  $120^\circ$  for phase-b and  $240^\circ$  for phase-c [32]. The general representation of shifted carrier signals with modulating signals is shown in Figure 8.

The proposed topology can operate in buck as well as boost modes depending upon the modulation signal ( $m_x$ ). For the proposed topology, the modulation index depends upon the grid voltage ( $v_g^x$ ), output DC voltage ( $V_{DC}$ ) and the gain of the rectifier ( $1/\beta$ ) (where  $\beta$  is 3 in this topology) and can be defined as:

$$m_x = \frac{v_g}{3V_{DC}}$$



**Figure 8.** General representation of shifted carrier signals with modulating signal for three-phase.

The proposed topology operates as buck as well as boost mode, depending upon the value of  $m_x$  as described herewith:

For the seven-level buck mode of operation:

$$\begin{aligned} \frac{1}{3}v_g^{\max} < V_{DC} < \frac{1}{2}v_g^{\max} \\ \text{i.e., } \frac{2}{3} < m_x < 1 \end{aligned} \tag{2}$$

For the five-level buck mode of operation:

$$\begin{aligned} \frac{1}{2}v_g^{\max} < V_{DC} < v_g^{\max} \\ \text{i.e., } \frac{1}{3} < m_x < \frac{2}{3} \end{aligned} \tag{3}$$

For the three-level boost mode of operation:

$$\begin{aligned} V_{DC} > v_g^{\max} \\ \text{i.e., } m_x < \frac{1}{3} \end{aligned} \tag{4}$$

Output voltage variation in terms of modulating signal ( $m_x$ ) is shown in Figure 9, for input RMS AC voltage of 170 V (i.e., the peak value of 240 V).

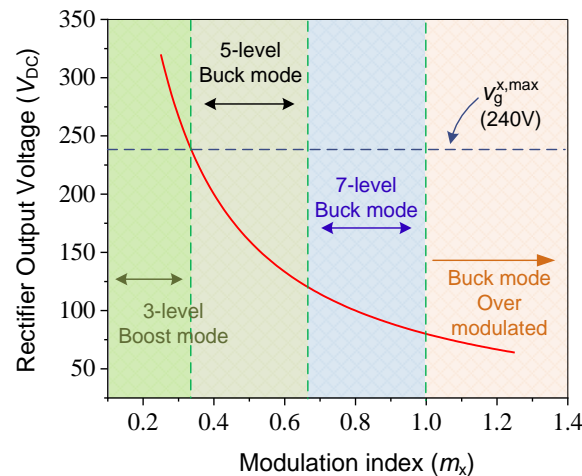


**Figure 9.** Variation in the output DC voltage with respect to the modulation index for the proposed multilevel rectifier.

### 3.2. Controller Design

Figure 10 depicts the principle of the control system employed for the proposed rectifier so as to achieve PFC and regulation of the output DC voltage. This control diagram has two feedback loops: one that is based on the output voltage and is compared to the reference value ( $V_{DC}^*$ ) imposed by the load's operating circumstances [23]; and second, a feedback loop which takes over the real-time phase currents and synthesizes the output signals corresponding to the two axes currents viz.  $i_d$  and  $i_q$ .

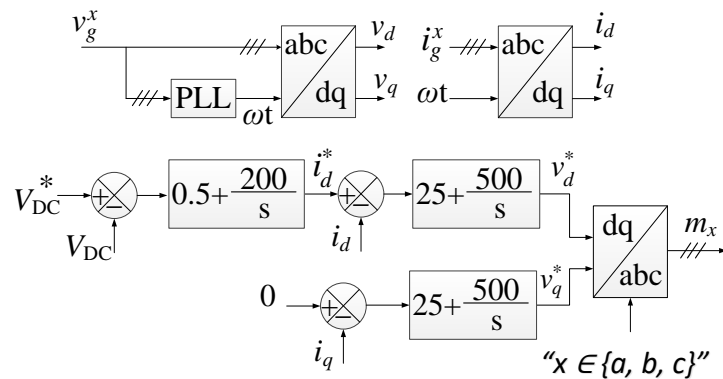


Figure 10. Generated reference signals by three-phase voltage and current controller.

The instantaneous angle ( $\omega t$ ) value that determines the rotating reference d-q position, as shown in Figure 10, is used by the axis transformation block. The  $i_d$  and  $i_q$  values of instantaneous signals are compared to the reference values  $i_d^*$  and  $i_q^*$  [33]. For the power factor to be near unity, the necessary condition would be  $i_q = 0$ . The PI controllers receive the signals generated by the comparators. In addition, reverse transformation is used to convert the two-phase quantities into three-phase quantities. At this state, the sinusoidal signals are the modulating signals ( $m_x, x \in \{a, b, c\}$ ) for the PWM pulse generator.

### 4. Comparative Analysis with Existing PFC Rectifiers

The proposed topology is capable of single/three-phase buck AC-to-DC conversion. A comparative analysis of multilevel PFC rectifier topologies classified as:

1. Single-phase PFC rectifier with buck and boost mode of operation (summarized in Table 3);
2. Three-phase PFC rectifier (summarized in Table 4).

Table 3. Comparison of proposed work with single phase buck and boost rectifier topology.

Parameters	Boost Topologies				Buck Topologies		
	H-Bridge [9]	NPC [19]	FC [20]	CHB [28]	[29]	[30]	Proposed
$N_L$	3	5	5	5	5	9	7
$N_s$	4	8	8	8	6	8	16
$N_D$	0	4	0	0	0	0	0
$N_C$	1	2	3	2	2	3	5
PIV	1	1	1	1	2	4	1
Gain ( $1/\beta$ )	1	1	1	0.5	0.5	0.25	1/3
$N_{Vs}$	2	2	2	3	3	4	2
$N_{Cs}$	1	1	1	1	1	4	1

$N_L$ : Number of levels,  $N_s$ : Number of switches,  $N_D$ : Number of diodes,  $N_C$ : Number of capacitors, PIV: Peak inverse voltage,  $N_{Vs}$ : Number of voltage sensors,  $N_{Cs}$ : Number of current sensors.

**Table 4.** Comparative analysis with existing three-phase PFC rectifier topologies.

References	$N_L$	$N_S$	$N_D$	$N_C$	Gain ( $1/\beta$ )	Bidirectional Capability	Output Voltage
[21]	5	18	0	2	1	Yes	Boost
[11]	5	12	0	2	2	Yes	Boost
[22]	5	12	0	4	1	Yes	Boost
[23]	5	6	24	12	1	No	Boost
[24]	9	12	24	8	1	No	Boost
[25]	9	12	12	8	1	No	Boost
[27]	9	24	0	4	1	Yes	Boost
[26]	13	54	0	2	1	Yes	Boost
Proposed	7	24	0	7	1/3	Yes	Buck

$N_L$ : Number of levels,  $N_S$ : Number of switches,  $N_D$ : Number of diodes,  $N_C$ : Number of capacitors.

The proposed switched-capacitor-based multilevel rectifier offers a buck output voltage, which is most suitable for an EV charging application. It is a novel approach to achieving buck output voltage in multilevel topologies. Table 3 compares the proposed topology to conventional single-phase multilevel rectifiers such as the H-bridge (HB) [9], neutral point clamped (NPC) [19], and flying capacitors (FC) [20]. These topologies have fewer components, but they have a unity voltage gain, making them boost rectifiers. Existing multilevel buck rectifiers proposed in [28–30] are compared to the proposed single-phase topology. These topologies are buck rectifiers with multiple output voltages. Different characteristics are compared, such as the number of levels ( $N_L$ ), switches ( $N_S$ ), diodes ( $N_D$ ), capacitors ( $N_C$ ), peak inverse voltage (PIV), voltage sensors ( $N_{VS}$ ), current sensors ( $N_{CS}$ ) and voltage gain. Power switches with PIV equal to double the output DC voltage are required in the [29] topology, as are additional voltage sensors. Similarly, topology in [30] necessitates power switches with PIV equivalent to four times the output DC voltage, as well as a large number of voltage and current sensors. These topologies have comparable drawbacks, such as difficulties balancing capacitor voltages, which is only attainable under balanced load conditions. Table 4 shows the comparison of the proposed topology with a three-phase conventional rectifier, i.e., NPC, T-type and FC based. These PFC rectifiers yield high voltage gain and achieve a boosted output voltage. The proposed work is also compared with existing multilevel three-phase topologies. This study is also based on the  $N_L$ ,  $N_S$ ,  $N_D$ ,  $N_C$ , Gain ( $1/\beta$ ) and the possibility of bidirectional power flow, which is possible to operate as a V2G mode and a buck or boost output voltage.

All compared items aforementioned are listed in Table 4. It indicates that the proposed seven-level buck rectifier has the advantages of simple structure and buck mode capability. Overall, it is a competitive circuit to implement EV charging infrastructure, mainly on account of the buck mode of operation and capability of bidirectional power flow. The conventional PFC rectifiers implemented in [11,21,22] are all specified for five-level boost operation with bidirectional power flow. To increase the levels in these converters, the number of power devices increases significantly. In the topology proposed in [23], the number of switches is low, but the number of power diodes is very high. It is useful for high voltage applications with unidirectional power flow only. The topologies discussed in [24,25] are conceptualized for a nine-level boost operation. As evident from Table 4, the number of switches is low but requires a large number of diodes. Moreover, these are not applicable for a bidirectional power flow. Both the structures presented in [26,27] operate with boost mode and offer a possibility of bidirectional power flow. The topology presented in [26] is modular and is implemented for a higher number of levels with the parallel use of active neutral point clamped (ANPC) modules. However, in this case, the number of devices is very high, increasing the rectifier controller complexity. Hence, it can be safely

concluded that the topology proposed in this work is highly competent with considerations of three-phase seven-level buck operation with bidirectional power flow.

## 5. Experimental Results

To evaluate the proposed three-phase buck rectifier and its closed-loop control, a laboratory setup was created utilizing discrete power switches MOSFETs (SiHG47N6) and an appropriate gate driver IC (Si82071AB-IS). A hall-effect-based voltage sensor (LEM LV25-P) and current sensor (HE025T01) with suitable power conditioning were used to sense the output voltage and input current. OPAL-RT OP4510, which connects with the hardware via MATLAB/Simulink on the host computer and generates the MOSFET gate pulses was used as a real-time controller. A photograph of the laboratory setup for validation of the proposed three-phase rectifier is shown in Figure 11. The controller and switching mechanism were developed using a 10  $\mu$ s sampling period. A three-phase 170 V RMS was used as an AC input, with the output DC voltages being 100 V (in buck mode). Table 5 summarizes the parameters used in the experiment. Sudden changes in the DC load and the output reference voltage were used to assess the system's performance in both steady-state and dynamic scenarios.

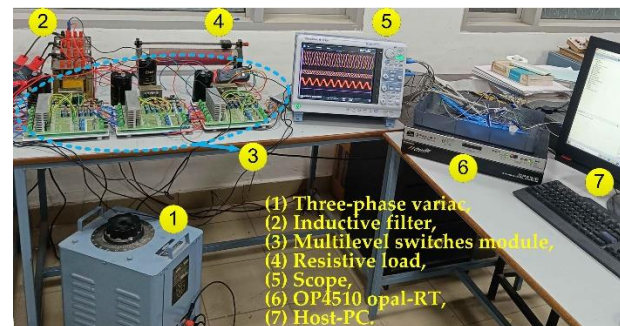


**Figure 11.** Photograph of the laboratory setup for validation of the proposed three-phase rectifier.

**Table 5.** Parameters for experimental verification of the proposed multilevel rectifier.

Parameters	Value	Unit
Input voltage	170 V for three-phase and 230 V for single-phase	V (RMS)
Input grid frequency	50	Hz
Filter inductor	4	mH
Capacitors (ALF80C162DF200)	1600	$\mu$ F
Switching frequency	10	kHz
DC load	10, 20, 30	$\Omega$
Output DC voltage	100 V for three-phase and 120 V for single-phase	V
Battery	48 V, 30 AH Lithium-ion ferrous phosphate	
Semiconductor switches	SiHG47N6	
Gate driver IC	Si82071AB-IS	
Hall effect voltage sensor	LEM LV25-P	
Current sensor	HE025T01	

Experimental results are taken with two scenarios, with a resistive load and another with an EV battery charging for a single/three-phase. When the rectifier converts 240 V three-phase peak AC (170 VRMS) to 100 V<sub>DC</sub> (in buck mode) and feeds it to the resistive

load ( $R_o = 10 \Omega$ ) with a 10 A load current, the steady-state results are achieved, as shown in Figure 12. Because the input current ( $i_g^x$ ) is sinusoidal and in phase with the input grid voltage ( $v_g^x$ ), the input power factor is maintained at unity.

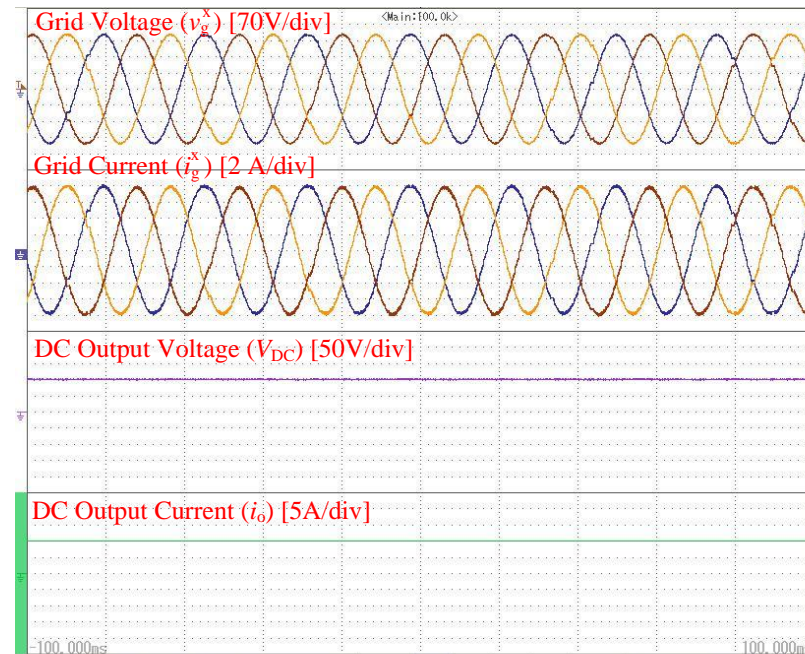


Figure 12. Steady-state experimental results in buck mode operation of the proposed rectifier.

As previously described, the proposed topology can also work in boost mode. Figure 13 shows the steady-state operation where the output voltage is regulated at 280 V (in boost mode with a wide output range) and feeds it to the resistive load ( $R_o = 30 \Omega$ ) with a 3 A load current. In this mode of operation, the grid voltages ( $v_g^x$ ) and grid currents ( $i_g^x$ ) are in phase.

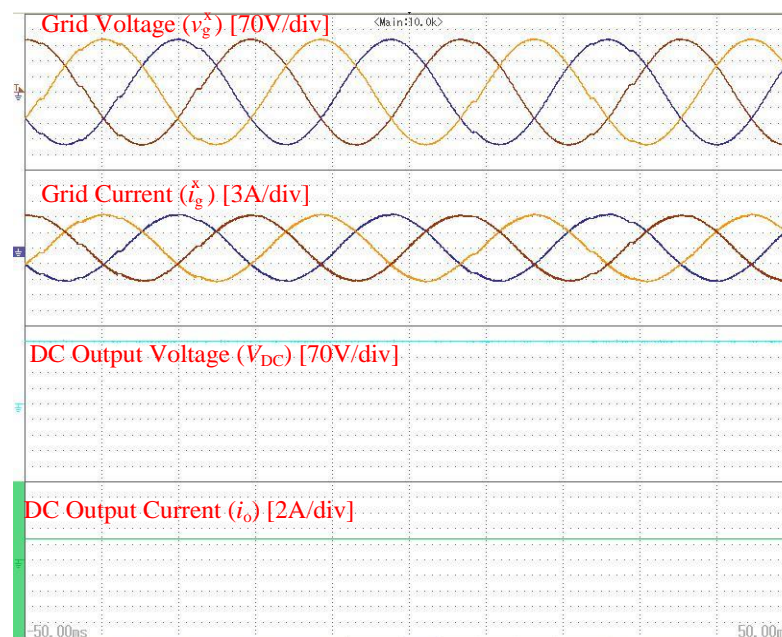


Figure 13. Steady-state experimental waveforms in the boost mode operation of the proposed rectifier.

The proposed multilevel rectifier operates in buck mode of operation. In the input, terminals of the rectifier generate four-level as a pole voltage ( $V_{xn}$ ) with levels of  $0, +V_{DC}, +2 V_{DC}, +3 V_{DC}$ . Moreover, seven-level is generated as a line voltage ( $V_{ab}, V_{bc}, V_{ca}$ ) with

levels of  $+3 V_{DC}$ ,  $+2 V_{DC}$ ,  $+V_{DC}$ ,  $0$ ,  $-V_{DC}$ ,  $-2 V_{DC}$  and  $-3 V_{DC}$  which improves the harmonic profile of the grid current and reduces the filter size. Three-phase pole voltages and line voltages are shown in Figure 14.

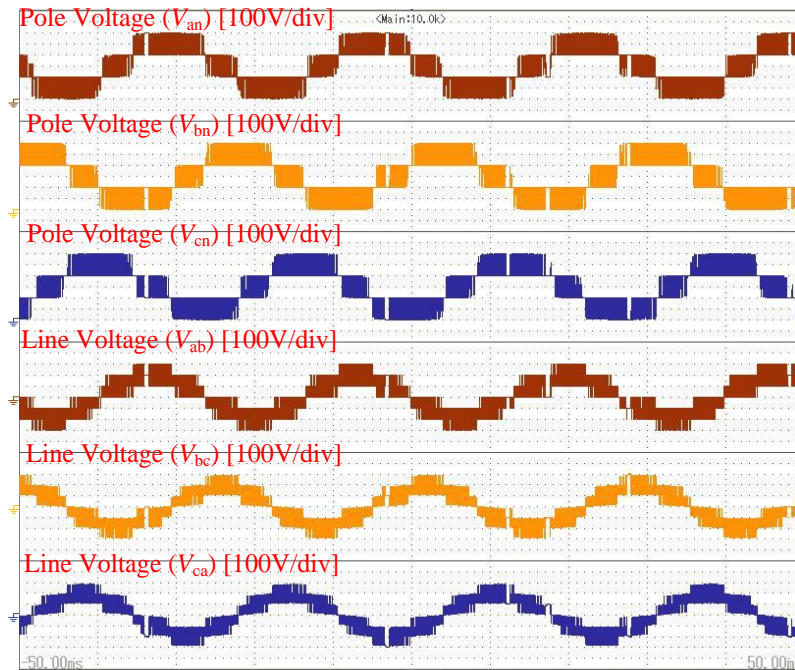


Figure 14. Experimental waveforms show four-level pole voltages and seven-level line voltages.

An experiment was carried out to validate the proposed rectifier’s dynamic performance. With a sudden 50% reduction in the load resistance ( $R_o$ ), raising the load current by a factor of two, the load voltage instantly stabilizes at 100 V. In addition, as indicated in Figure 15, the rectifier maintains a unity power factor. In another case, the output DC reference voltage increases. As seen in Figure 16, the reference voltage varies by 30%, causing  $V_{DC}$  and  $i_o$  to fluctuate abruptly. The load voltage stayed constant at 130 V, and the rectifier operated at a unity power factor.

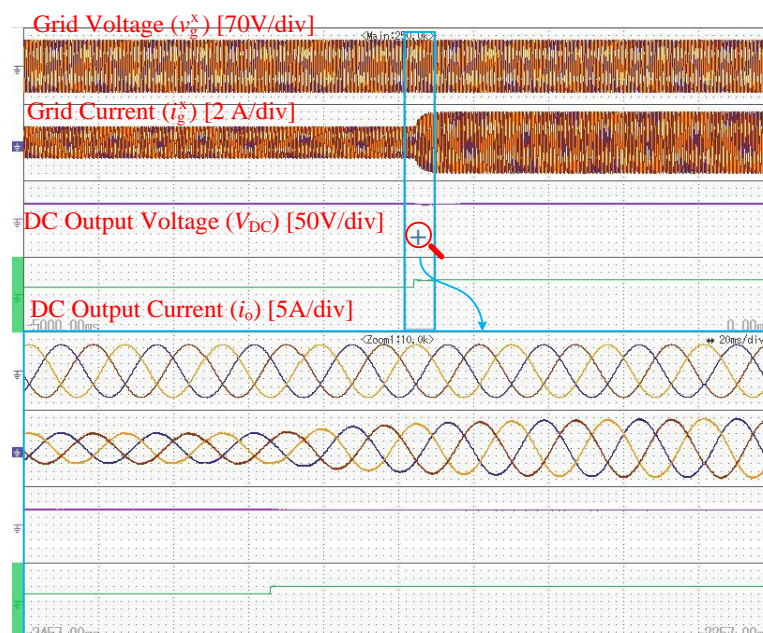


Figure 15. Experimental results during 50% load change.

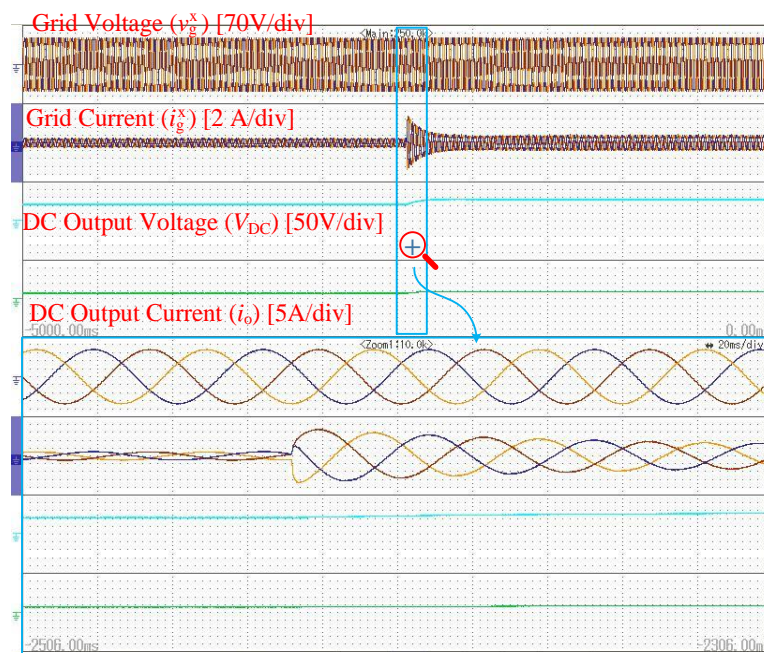


Figure 16. Experimental results during 30% rise in the DC voltage reference.

A power electronics interface consisting of the proposed PFC rectifier and a typical buck–boost DC-DC converter is constructed to illustrate application in three-phase charging. The ratings are based on a three-phase input voltage of 170 VRMS at 50 Hz and a rectifier output DC voltage of 100 V. The voltage and current of the battery are 48 V and 16 A, respectively. Figure 17 depicts the battery charging, where the waveforms indicate that the grid voltage and current are in phase. The rectifier’s output voltage is controlled to 100 V<sub>DC</sub> and further regulated to battery voltage 48 V using a DC-DC converter.

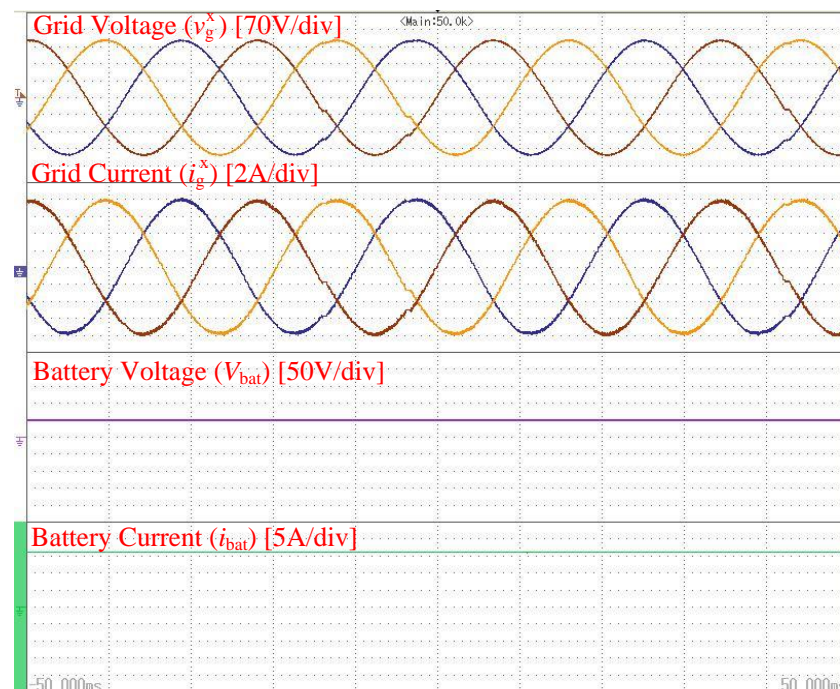
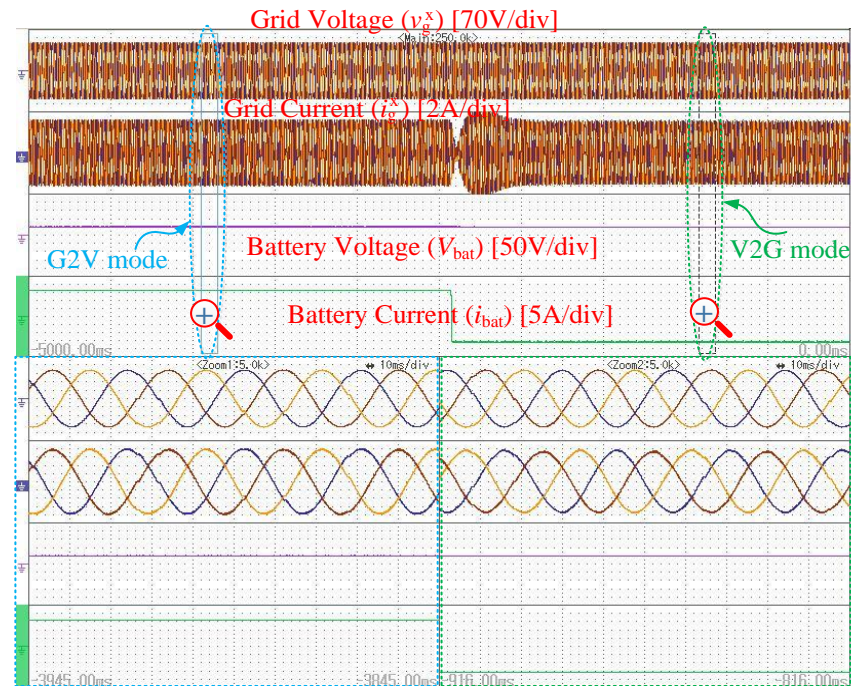


Figure 17. Experimental waveforms for three-phase battery charging.

The V2G mode allows the injection of battery energy back into the grid. Grid-to-vehicle (G2V) charging and vehicle-to-grid (V2G) discharging modes are available for EVs.

The interface must be capable of bidirectional power flow in order to use V2G mode. The proposed topology supports charging as well as discharging in its three-phase variants. Figure 18 depicts experiments in both modes of operation (G2V and V2G). When an abrupt change in the flow of the battery current is directed, the battery current is seen to be reversed. In this case, the grid current is  $180^\circ$  out of phase with the grid voltage.



**Figure 18.** Bidirectional power flow with the proposed rectifier for V2G application.

In single-phase, Figures 19 and 20 show the EV battery charging and bidirectional operation. A power electronics interface consisting of the proposed single-phase PFC rectifier and a standard buck-boost DC-DC converter is created to demonstrate application in single-phase EV charging. The voltage and current of the battery are 48 V and 25 A, respectively. The waveforms of the battery charging are shown in Figure 19, which indicates that the grid voltage and current are in phase and achieve a unity power factor. The rectifier's output voltage is set to 120 volts DC and then regulated to 48 volts using a DC-DC converter. The V2G mode allows injecting battery energy back into the grid. In the single-phase operation, EVs may charge and discharge using grid-to-vehicle (G2V) and vehicle-to-grid (V2G) modes. The experimental results of both modes of operation (G2V and V2G) are illustrated in Figure 20.

A total harmonic distortion (THD) and input power factor (IPF) are estimated for the proposed seven-level rectifier, and comparisons are performed with the conventional boost rectifier. The following parameters were used for the THD and IPF calculations: carrier frequency of 10 kHz, input AC voltage of 325, output DC voltage of 400 V for conventional topologies, and 120 V for the proposed topology. When the proposed topology is compared to the others in terms of THD (vs. load) (Figure 21) and Input Power Factor (IPF) (vs. load) (Figure 22), the proposed topology has a low THD due to the seven-level topology and achieves a high IPF value. Figure 23 depicts the distribution of power losses for the proposed IPF rectifier using the single-phase parameters listed in Table 5. With an overall efficiency of 95.46%, the total loss (switching loss and conduction loss) in power switches is 46 W. Modeling the single-phase converters and their control in Plexim PLECS software gives the proposed topology's power loss distribution.

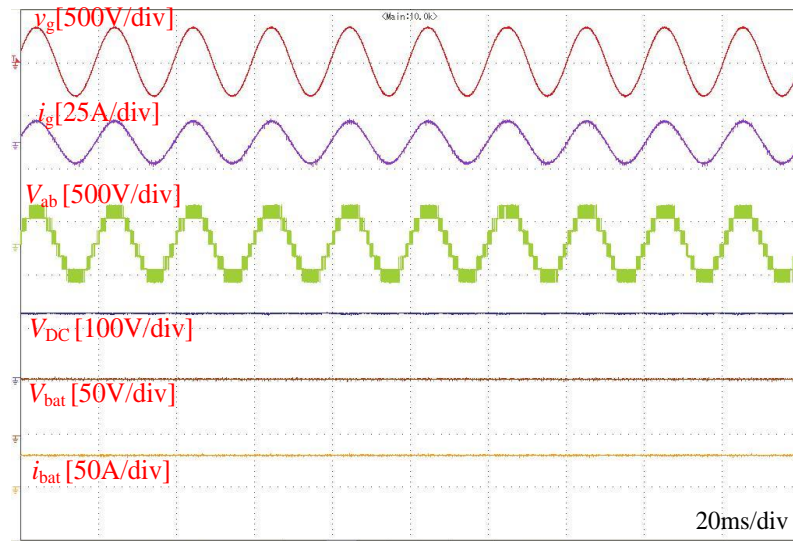


Figure 19. Single phase battery charging with unity power factor.

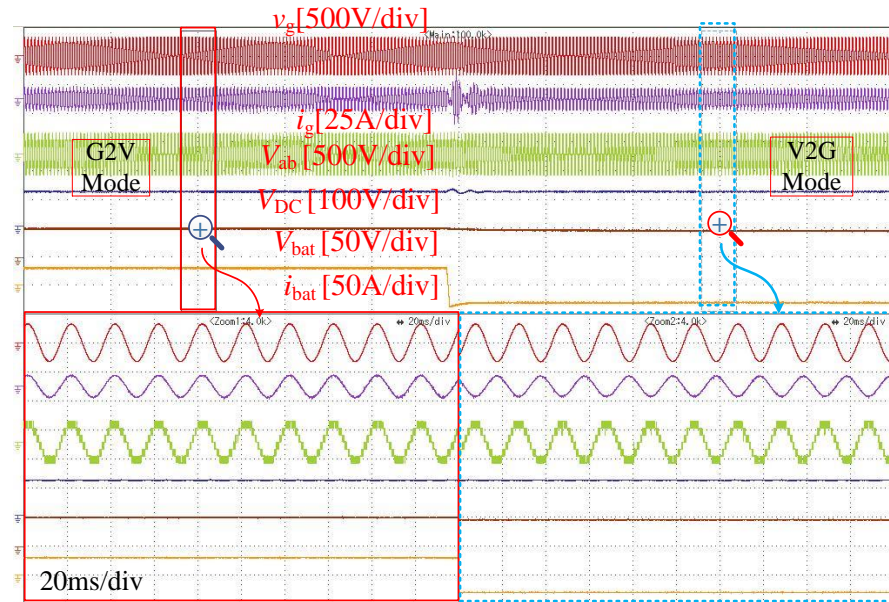


Figure 20. Single-phase EV charging (G2V) and power injected back to the grid (V2G) with unity power factor.

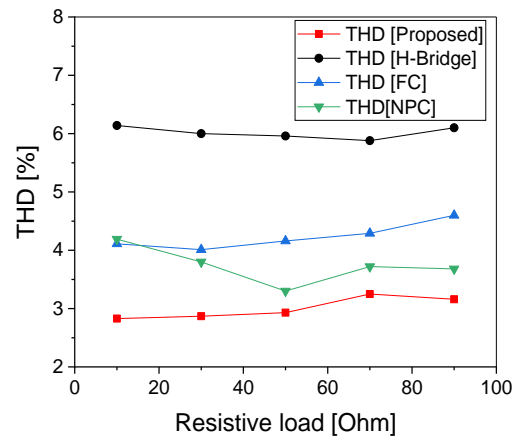


Figure 21. Comparison of THD vs. load with conventional rectifier.

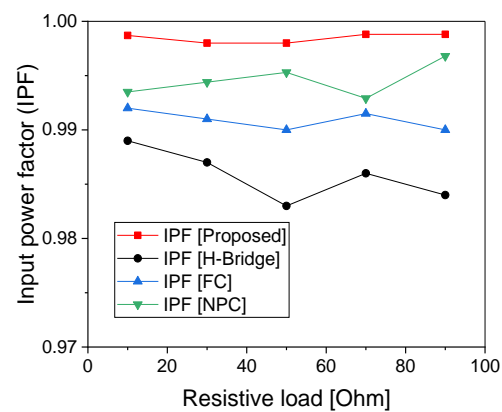


Figure 22. Comparison of IPF vs. load with conventional rectifier.

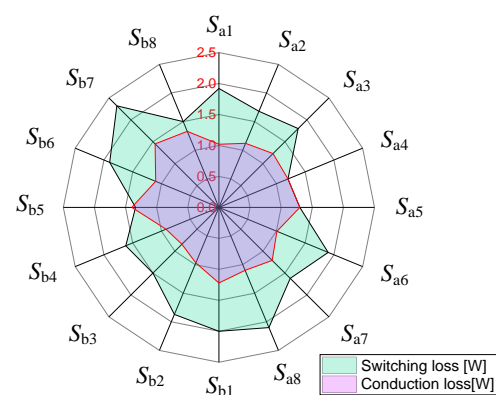


Figure 23. Distribution of power loss for 1015 W input power, power loss 46 W and efficiency is 95.46%.

## 6. Conclusions

This paper offers a new multilevel single/three-phase buck PFC rectifier based on SCs suitable for EV charging and V2G operation. The voltage is balanced using LSPWM and a voltage and current controller. The performance of the three-phase AC input of 170 V RMS and DC output of 100 V for various dynamic situations has been tested using a proto-model implementation. The following findings have been reached:

- It synthesizes input into four levels as a pole voltage and seven levels as a line voltage, enhancing the waveform's harmonic profile.
- It has a wide output voltage range and can work in buck and boost mode, making it suitable for many applications.
- The proposed rectifier is suitable for EV battery charging due to its buck mode of operation.
- It operates in continuous conduction mode (CCM), which eliminates the need for large filters.
- It has an inbuilt self-voltage balancing capability that does not require extra circuitry.
- It is capable of bidirectional power flow.
- It achieves an efficiency of 95.46%, low THD and high IPF compared to the conventional multilevel rectifier.

**Author Contributions:** Conceptualization, A.J. and K.K.G.; methodology, A.J.; software, A.J.; validation, A.J., K.K.G., S.K.J., P.B. and H.V.; formal analysis, A.J.; investigation, A.J.; resources, A.J.; data curation, A.J.; writing—original draft preparation, A.J.; writing—review and editing, A.J., K.K.G. and H.V.; visualization, A.J.; supervision, K.K.G., S.K.J., P.B. and H.V.; project administration, S.K.J. and P.B.; funding acquisition, H.V. and P.B. All authors have read and agreed to the published version of the manuscript.

**Funding:** This work was funded by the Ministry of Electronics and Information Technology (MeitY), Government of India, for the financial support to this work under National Mission on Power Electronics Technology (NaMPET-III), Project No. NaMPET-III/SP25/NH-EXP-05. This work was also supported by Thapar Institute of Engineering and Technology, Patiala, India under the Grant No. TU/DORSP/57/7215.

**Institutional Review Board Statement:** Not applicable.

**Informed Consent Statement:** Not applicable.

**Data Availability Statement:** Not applicable.

**Acknowledgments:** Thanks to the editors and reviewers for their careful review, constructive suggestion, and reminding, which helped improve the quality of the paper.

**Conflicts of Interest:** The authors declare no conflict of interest.

## References

1. Chan, C.C. The State of the Art of Electric and Hybrid Vehicles. *Proc. IEEE* **2002**, *90*, 247–275. [[CrossRef](#)]
2. Yilmaz, M.; Krein, P.T. Review of Battery Charger Topologies, Charging Power Levels, and Infrastructure for Plug-in Electric and Hybrid Vehicles. *IEEE Trans. Power Electron.* **2013**, *28*, 2151–2169. [[CrossRef](#)]
3. Su, W.; Eichi, H.; Zeng, W.; Chow, M.Y. A Survey on the Electrification of Transportation in a Smart Grid Environment. *IEEE Trans. Ind. Inform.* **2012**, *8*, 1–10. [[CrossRef](#)]
4. Kisacikoglu, M.C.; Kesler, M.; Tolbert, L.M. Single-Phase on-Board Bidirectional PEV Charger for V2G Reactive Power Operation. *IEEE Trans. Smart Grid* **2015**, *6*, 767–775. [[CrossRef](#)]
5. Kumar, V.; Yi, K. Single-Phase, Bidirectional, 7.7 KW Totem Pole On-Board Charging/Discharging Infrastructure. *Appl. Sci.* **2022**, *12*, 2236. [[CrossRef](#)]
6. Kisacikoglu, M.C.; Ozpineci, B.; Tolbert, L.M. EV/PHEV Bidirectional Charger Assessment for V2G Reactive Power Operation. *IEEE Trans. Power Electron.* **2013**, *28*, 5717–5727. [[CrossRef](#)]
7. Madawala, U.K.; Thrimawithana, D.J. A Bidirectional Inductive Power Interface for Electric Vehicles in V2G Systems. *IEEE Trans. Ind. Electron.* **2011**, *58*, 4789–4796. [[CrossRef](#)]
8. Tariq, A. A Modified Battery Charger with Power Factor Correction for Plug-In Electrical Vehicles. In Proceedings of the The 1st International Conference on Energy, Power and Environment, Basel, Switzerland, 9 March 2022; p. 103.
9. Rothmund, D.; Guillod, T.; Bortis, D.; Kolar, J.W. 99.1% Efficient 10 KV SiC-Based Medium-Voltage ZVS Bidirectional Single-Phase PFC AC/DC Stage. *IEEE J. Emerg. Sel. Top. Power Electron.* **2019**, *7*, 779–797. [[CrossRef](#)]
10. Haller, S.; Alam, M.F.; Bertilsson, K. Reconfigurable Battery for Charging 48 V EVs in High-Voltage Infrastructure. *Electronics* **2022**, *11*, 353. [[CrossRef](#)]
11. Lee, J.S.; Choi, U.M.; Lee, K.B. Comparison of Tolerance Controls for Open-Switch Fault in a Grid-Connected T-Type Rectifier. *IEEE Trans. Power Electron.* **2015**, *30*, 5810–5820. [[CrossRef](#)]
12. Ramakrishnan, H.; Rangaraju, J. *Power Topology Considerations for Electric Vehicle Charging Stations*; Texas Instruments: Dallas, TX, USA, 2020.
13. Lee, S.S. Single-Stage Switched-Capacitor Module (S3CM) Topology for Cascaded Multilevel Inverter. *IEEE Trans. Power Electron.* **2018**, *33*, 8204–8207. [[CrossRef](#)]
14. Soeiro, T.B.; Friedli, T.; Kolar, J.W. Swiss Rectifier—A Novel Three-Phase Buck-Type PFC Topology for Electric Vehicle Battery Charging. In Proceedings of the 2012 Twenty-Seventh Annual IEEE Applied Power Electronics Conference and Exposition (APEC), Orlando, FL, USA, 5–9 February 2012; pp. 2617–2624.
15. Xie, X.; Zhao, C.; Zheng, L.; Liu, S. An Improved Buck PFC Converter with High Power Factor. *IEEE Trans. Power Electron.* **2013**, *28*, 2277–2284. [[CrossRef](#)]
16. Choi, H. Interleaved Boundary Conduction Mode (BCM) Buck Power Factor Correction (PFC) Converter. *IEEE Trans. Power Electron.* **2013**, *28*, 2629–2634. [[CrossRef](#)]
17. Wu, X.; Yang, J.; Zhang, J.; Qian, Z. Variable On-Time (VOT)-Controlled Critical Conduction Mode Buck PFC Converter for High-Input AC/DC HB-LED Lighting Applications. *IEEE Trans. Power Electron.* **2012**, *27*, 4530–4539. [[CrossRef](#)]
18. Teixeira, C.A.; Holmes, D.G.; McGrath, B.P. Single-Phase Semi-Bridge Five-Level Flying-Capacitor Rectifier. *Proc. IEEE Trans. Ind. Appl.* **2013**, *49*, 2158–2166. [[CrossRef](#)]
19. Zhou, D.; Jiang, C.; Quan, Z.; Li, Y. Vector Shifted Model Predictive Power Control of Three-Level Neutral-Point-Clamped Rectifiers. *IEEE Trans. Ind. Electron.* **2020**, *67*, 7157–7166. [[CrossRef](#)]
20. Khazraei, M.; Sepahvand, H.; Ferdowsi, M.; Corzine, K.A. Hysteresis-Based Control of a Single-Phase Multilevel Flying Capacitor Active Rectifier. *IEEE Trans. Power Electron.* **2013**, *28*, 154–164. [[CrossRef](#)]
21. Najjar, M.; Kouchaki, A.; Nielsen, J.; Dan Lazar, R.; Nymand, M. Design Procedure and Efficiency Analysis of a 99.3% Efficient 10 KW Three-Phase Three-Level Hybrid GaN/Si Active Neutral Point Clamped Converter. *IEEE Trans. Power Electron.* **2022**, *37*, 6698–6710. [[CrossRef](#)]

22. Syu, Y.L.; Liao, Z.; Fu, N.T.; Liu, Y.C.; Chiu, H.J.; Pilawa-Podgurski, R.C.N. Design and Control of a High Power Density Three-Phase Flying Capacitor Multilevel Power Factor Correction Rectifier. In Proceedings of the Conference Proceedings—IEEE Applied Power Electronics Conference and Exposition (APEC), Phoenix, AZ, USA, 14–17 June 2021; pp. 613–618.
23. Cortez, D.F.; Barbi, I. A Three-Phase Multilevel Hybrid Switched-Capacitor PWM PFC Rectifier for High-Voltage-Gain Applications. *IEEE Trans. Power Electron.* **2016**, *31*, 3495–3505. [[CrossRef](#)]
24. Mukherjee, D.; Kastha, D. A Reduced Switch Hybrid Multilevel Unidirectional Rectifier. *IEEE Trans. Power Electron.* **2019**, *34*, 2070–2081. [[CrossRef](#)]
25. Itoh, J.I.; Noge, Y.; Adachi, T. A Novel Five-Level Three-Phase PWM Rectifier with Reduced Switch Count. *IEEE Trans. Power Electron.* **2011**, *26*, 2221–2228. [[CrossRef](#)]
26. Abarzadeh, M.; Khan, W.A.; Weise, N.; Al-Haddad, K.; El-Refaie, A.M. A New Configuration of Paralleled Modular ANPC Multilevel Converter Controlled by an Improved Modulation Method for 1 MHz, 1 MW EV Charger. *IEEE Trans. Ind. Appl.* **2021**, *57*, 3164–3178. [[CrossRef](#)]
27. Yalla, N.; Babu, N.A.; Agarwal, P. A New Three-Phase Multipoint Clamped 5L-HPFC with Reduced PSD Count and Switch Stress. *IEEE Trans. Ind. Electron.* **2020**, *67*, 2532–2543. [[CrossRef](#)]
28. Dell’Aquila, A.; Liserre, M.; Monopoli, V.G.; Rotondo, P. Overview of PI-Based Solutions for the Control of DC Buses of a Single-Phase H-Bridge Multilevel Active Rectifier. *IEEE Trans. Ind. Appl.* **2008**, *44*, 857–866. [[CrossRef](#)]
29. Vahedi, H.; Al-Haddad, K. A Novel Multilevel Multioutput Bidirectional Active Buck Pfc Rectifier. *IEEE Trans. Ind. Electron.* **2016**, *63*, 5442–5450. [[CrossRef](#)]
30. Babaie, M.; Al-Haddad, K. A Novel Single-Phase Triple-Output Active Buck Rectifier Using Nine-Level Packed E-Cell Converter. In Proceedings of the SEST 2021—4th International Conference on Smart Energy Systems and Technologies, Vaasa, Finland, 6–8 September 2021.
31. Kazmierkowski, M.P.; Malesani, L. Current Control Techniques for Three-Phase Voltage-Source Pwm Converters: A Survey. *IEEE Trans. Ind. Electron.* **1998**, *45*, 691–703. [[CrossRef](#)]
32. Carrara, G.; Gardella, S.; Marchesoni, M.; Salutari, R.; Sciutto, G. A New Multilevel PWM Method: A Theoretical Analysis. *IEEE Trans. Power Electron.* **1992**, *7*, 497–505. [[CrossRef](#)]
33. Zmood, D.N.; Holmes, D.G. Stationary Frame Current Regulation of PWM Inverters with Zero Steady State Error. In Proceedings of the PESC Record—IEEE Annual Power Electronics Specialists Conference, Charleston, SC, USA, 1 July 1999; Volume 2, pp. 1185–1190.